

# Characterization of the ternary compounds $\text{AgGaTe}_2$ and $\text{AgGa}_5\text{Te}_8$

C. JULIEN, I. IVANOV, A. KHELFA

*Laboratoire de Physique des Solides, associé au CNRS, Université Pierre et Marie Curie  
4 place Jussieu, 75252 Paris Cédex 05, France*

F. ALAPINI, M. GUITTARD

*Laboratoire de Chimie Physique Minérale et Bio-Inorganique Faculté de Pharmacie,  
Université Paris XI Rue J.-B. Clément, 92296 Chatenay-Malabry, France*

Optical and electrical properties of ternary compounds in the Ag–Ga–Te system are reported. Vibrational properties of  $\text{AgGaTe}_2$  and  $\text{AgGa}_5\text{Te}_8$  single crystals were studied using Raman scattering and infrared absorption spectroscopy. Long-wavelength spectra are analysed and the symmetry of lattice modes are reported. The semiconducting character of Ag–Ga–Te compounds is confirmed by conductivity measurements.

## 1. Introduction

Compounds of the I–III–VI family are generally semiconducting materials which usually crystallize in the chalcopyrite structure but occasionally some of them take up the disordered zinc-blende structure [1]. These ternary compounds similar to  $\text{A}^{\text{II}}\text{B}^{\text{VI}}$  compounds have a small energy gap and proved to be of great interest as nonlinear optical materials [2, 3].

$\text{AgGaTe}_2$  was prepared for the first time by Hahn *et al.* [4] who showed that this compound crystallizes within the chalcopyrite structure and belongs to space group I42d. The properties of this compound have been studied as functions of temperature and pressure [5–14] and solid solutions have been described to be in the vicinity of  $\text{AgGaTe}_2$  [15].

Information on the phase diagram of the  $\text{Ag}_2\text{Te}$ – $\text{Ga}_2\text{Te}_3$  system is rather limited as yet although Palatnick and Belova [8–10] have reported the existence of  $\text{AgGa}_5\text{Te}_8$  and solid solutions in the vicinity of  $\text{Ga}_2\text{Te}_3$ . Similar studies have been made by Krämer *et al.* [16] and Guittard *et al.* [15, 17–18] who have mentioned the existence of  $\text{Ag}_9\text{GaTe}_6$  and another non-stoichiometric phase in the  $\text{Ag}_2\text{Te}$ – $\text{Ga}_2\text{Te}_3$  system. However, there is a lack of information on electrical and optical properties of these materials because of the difficulty in growing large, good quality crystals.

The purpose of this communication is to examine some properties of compounds of the Ag–Ga–Te ternary system. A description of the  $\text{Ag}_2\text{Te}$ – $\text{Ga}_2\text{Te}_3$  quasi-binary phase diagram is presented and the role of oxygen in the creation of phases is discussed. Optical and electrical characterizations of  $\text{AgGaTe}_2$  and  $\text{AgGa}_5\text{Te}_8$  have been performed using Raman scattering, far-infrared absorption spectroscopy and resistivity measurements.

## 2. Experimental procedure

Samples in the  $\text{Ag}_2\text{Te}$ – $\text{Ga}_2\text{Te}_3$  system were prepared from telluride compounds, i.e.  $\text{Ga}_2\text{Te}_3$  and  $\text{Ag}_2\text{Te}$ , previously synthesized as reported by Guittard *et al.* [17]. Each synthesis was carried out in a sealed silica tube under vacuum which was heated slowly up to 1000 °C at a rate of 40 °C h<sup>-1</sup>. All the samples have been studied by differential thermal analysis and by X-ray diffraction using the Guinier–Lenné method.

Raman scattering and infrared absorption spectra were recorded at room temperature. In the Raman measurements a double-monochromator (model Jobin–Yvon U1000) equipped with holographic gratings and a GaAs-cathode photomultiplier tube (model RCA C31034) in photon-counting mode were used. An Ar<sup>+</sup> ion laser line at 514.5 nm with an output power of 20 mW was utilized as an excitation source. Raman spectra were recorded in the backscattering geometry with a spectral resolution of 3 cm<sup>-1</sup>.

Far-infrared (FIR) absorption spectra were recorded using a Bruker IFS113 vacuum Fourier transform interferometer equipped with a germanium bolometer cooled at 4.2 K, a 6 µm thick mylar beamsplitter, and a Hg light source. Each spectrum represented in the experimental results is an average over 64 scans recorded with a spectral resolution of 1 cm<sup>-1</sup>. FIR transmission spectra were recorded on samples ground and dispersed in solid paraffin wax. Pellets pressed at 500 hPa were used to get FIR spectra in the range 20–600 cm<sup>-1</sup> [19].

Electrical conductivity measurements were carried out in inert atmosphere (purified argon) using the five-probe technique. Silver painted spots provided ohmic contacts with the single crystals. Low-temperature measurements were performed between 77–300 K in a SMC-TBT gas-flow cryostat in which

the temperature was controlled using a Si-diode sensor.

### 3. Results and discussion

#### 3.1. Description of the phase diagram of the $\text{Ag}_2\text{Te}$ – $\text{Ga}_2\text{Te}_3$ system

Two descriptions of the phase diagram of  $\text{Ag}_2\text{Te}$ – $\text{Ga}_2\text{Te}_3$  are possible depending whether or not a slight amount of oxygen was present during the sample preparation. In order to clarify discrepancies reported in the literature three different procedures have been carried out as follows.

(1) The first synthesis procedure consists of a theoretical absence of oxygen. Special attention was focused on the growth of oxygen-free compounds using non-oxidized telluride materials and well-evacuated tubes.

(2) The second synthesis method consists of the synthesis of compounds with a slight quantity of oxygen which was intentionally introduced by a poor evacuation of the tubes and by oxidized telluride materials.

(3) The third synthesis method consists of the introduction of a small amount of gallium oxide into the melt, i.e. typically 1 mol %  $\text{Ga}_2\text{O}_3$ . These results are identical to those obtained with the second procedure. X-ray diffraction patterns exhibit lines due to  $\text{Ga}_2\text{O}_3$  showing that oxygen is present in small amounts.

When the growth is under oxygen-free conditions then the phase diagram is similar to that reported previously [18]. Three compounds were observed on the  $\text{Ag}_2\text{Te}$ – $\text{Ga}_2\text{Te}_3$  line (Fig. 1): (A)  $\text{Ag}_9\text{GaTe}_6$  which has a congruent melting point at  $710^\circ\text{C}$  and a polymorphic transformation at  $29^\circ\text{C}$ , being hexagonal on both sides of this temperature, (B)  $\text{AgGaTe}_2$  which is a tetragonal chalcopyrite-type phase and has a congruent melting point at  $710^\circ\text{C}$ , and (C) a lacunar phase  $\text{Ag}_x\text{Ga}_{(4-x)/3}\square_{(2-2x)/3}\text{Te}_2$  which is a solid solution for  $0.63 \leq x \leq 0.75$  with a peritectic decomposition at  $700^\circ\text{C}$ , has a stability domain between  $585$  and  $700^\circ\text{C}$ , and is an incongruent melting binary type. In addition there is a solid solution in the vicinity of  $\text{Ga}_2\text{Te}_3$  which has a cubic zinc-blende-type structure [18]. The end composition of this solid solution is  $\text{Ag}_{0.38}\text{Te}_{2.54}\square_{1.08}\text{Te}_4$  obtained in the absence of oxygen.

When compounds are grown in the presence of a slight quantity of oxygen, one observes different features as follows;

(1)  $\text{AgGaTe}_2$  possesses an incongruent melting point in good agreement with earlier works [8–10].

(2) A new stoichiometric compound  $\text{AgGa}_5\text{Te}_8$  (D) is formed in the presence of a slight amount of oxygen in the melt. The growth of this compound has been reported by two groups of workers [8, 17]. This compound has a tetragonal structure (space group  $\text{I}4_1/a$ ) with crystallographic parameters  $a = b = 0.8415$  nm and  $c = 4.7877$  nm. The resolution of this structure was difficult because the high value of the  $c$  parameter which could describe a zinc-blende superstructure with  $a = b = a_0 2^{1/2}$  and  $c = 8a_0$ .

(3) The congruency of the  $\text{Ag}_9\text{GaTe}_6$  is maintained and the existence of phase (C) is confirmed in a narrow

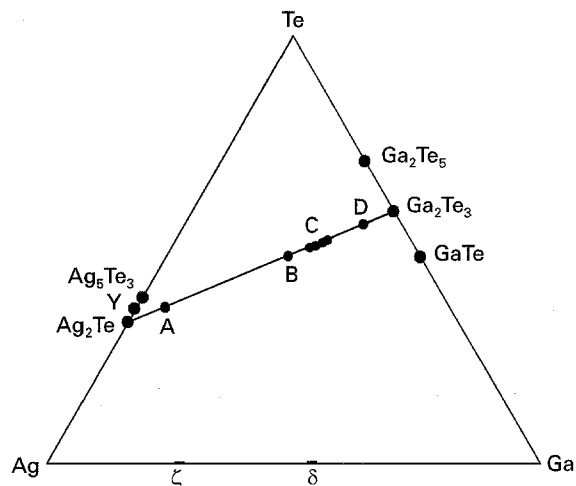


Figure 1 Local compositions in the ternary Ag–Ga–Te phase diagram. A:  $\text{Ag}_9\text{GaTe}_6$ , B:  $\text{AgGaTe}_2$ , C:  $\text{Ag}_x\text{Ga}_{(4-x)/3}\square_{(2-2x)/3}\text{Te}_2$  and D:  $\text{AgGa}_5\text{Te}_8$ .

temperature domain. Three eutectics and a peritectic are present.

#### 3.2. Optical properties

The long-wavelength optical modes in  $\text{AgGaTe}_2$  and  $\text{AgGa}_5\text{Te}_8$  crystals have been investigated using Raman scattering and infrared (IR) absorption measurements. The results are summarized in Table I.  $\text{AgGaTe}_2$  crystallizes within the chalcopyrite structure and has a unit cell which contains two formula units. According to the group theoretical analysis made by Kaminow *et al.* [20] there are 24 degrees of freedom and 21 optical modes of the centre of the Brillouin zone which can be presented as irreducible representations of the point group  $D_{2d}^{12}$

$$\Gamma = 1A_1 + 3B_1 + 3B_2 + 6E + 2A_2 \quad (1)$$

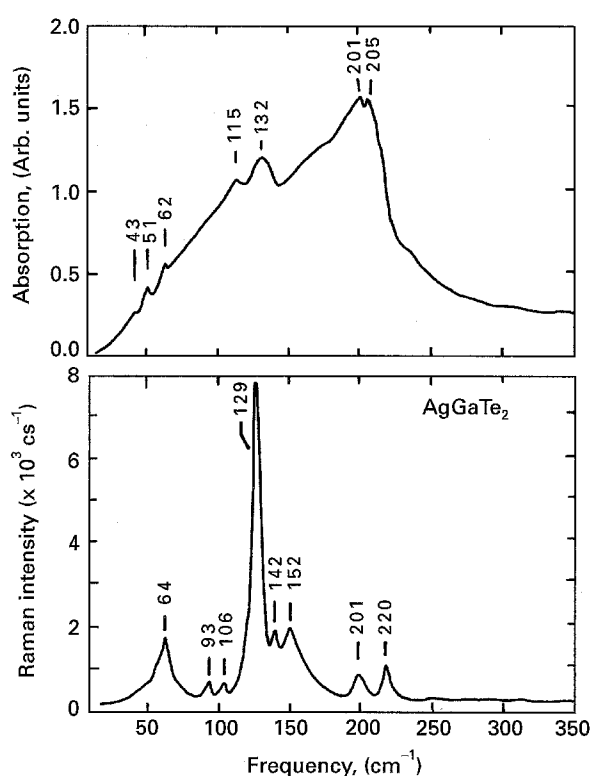
Here, three modes of symmetry  $B_2$  and six doubly degenerate modes of symmetry E are IR-active. These vibrations are also Raman-active together with the  $A_1$  and three  $B_1$  modes. The remaining two  $A_2$  modes are silent.

Fig. 2 shows the vibrational spectra of a  $\text{AgGaTe}_2$  single crystal. The Raman scattering spectrum exhibits eight bands and is dominated by a strong peak located at  $129\text{ cm}^{-1}$ . The chalcopyrite structure may be obtained from the zinc-blende structure by the ordering of two cations on to one sublattice. The lowering of symmetry gives rise to two distortions of this ideal structure. The resulting spectra for the chalcopyrite-type compounds exhibit, as expected, similar features to other compounds of the family [21–25].

Holah *et al.* [21] have given the displacement coordinates for the atomic vibrations from an analysis of the normal modes of the zinc-blende structure. Kanelis [25] has calculated the zone centre transverse optic-mode frequencies based on a valence field force model for ternary compounds  $\text{AgMX}_2$  (where  $M = \text{Ga, In}$  and  $X = \text{Se, Te}$ ). The computed values have been compared to the experimental data obtained by far-infrared reflection measurements.

TABLE I Results of the lattice mode analysis of  $\text{AgGaTe}_2$  and  $\text{AgGa}_5\text{Te}_8$  crystals. Frequencies are in  $\text{cm}^{-1}$ 

$\text{AgGaTe}_2$ Raman	IR	Assignment	$\text{AgGa}_5\text{Te}_8$ Raman	IR	Assignment
	43	$E^6$	37		$B_g$
	51	$B_g^3$	48		$B_g$
64	62	$B_{1,2}^3, E^5$	89	91	$E_g$
93		$B_1^2$	103		$B_g$
106				122	$A_u$
	115	$E^4$	125		$A_g$
129		$A_1$	139		$A_u$
142	132	$B_2^2$	141		$A_g$
152		$B_2^2$		173	$E_u$
201	201	$B_{1,2}^1, E^2$		201	$E_u$
	205	$E^1$	227	225	$E_g$
220		$B_1^1$		272	$E_u$


 Figure 2 Raman scattering and far-infrared absorption spectra of an  $\text{AgGaTe}_2$  single crystal recorded at room temperature.

The strongest mode in  $\text{AgGaTe}_2$  which appears at  $129 \text{ cm}^{-1}$  implies that the lattice vibration is based on the participation of only those metal ions whose tetrahedral environment is almost undisturbed. This band is attributed to the one totally symmetric  $A_1$  mode. Similar features have been reported by Holah *et al.* [21] who have observed that the  $A_1$  mode at  $295 \text{ cm}^{-1}$  gives rise to a much stronger Raman peak than any other in  $\text{AgGaS}_2$ . In the lattice of I-III-VI<sub>2</sub> compounds the trivalent metal ion is known to be in the centre of a nearly perfect tetrahedron formed by surrounding chalcogen ions [26]. Accordingly, the degeneracy of a strong polar mode is typical also of the other ternary compounds. For  $\text{AgGaTe}_2$  the frequency of the degenerate mode corresponds to a

frequency of  $201 \text{ cm}^{-1}$ . Evidently this mode also results from the vibration of the gallium ion with respect to the chalcogen ion.

The experimental frequencies for Raman-active modes can be compared with the predicted data of Kanellis [25]. The agreement between experimental results and calculated data are satisfactory except for the Raman-active modes of  $B_1$  symmetry. Examination of the influence of each parameter to the mode frequency shows that a more detailed description of the angular forces is needed in order to decrease this deviation because the slight distortion of the crystal structure.

$\text{AgGa}_5\text{Te}_8$  crystallizes within the scheelite structure with space symmetry group  $C_{4h}^6$ . There are 42 normal modes in the centre of the Brillouin zone which can be represented as irreducible representations [27]

$$\Gamma = 5A_g + 5B_g + 5E_g + 4A_u + 2B_u + 4E_u \quad (2)$$

Of these modes the  $A_u + B_u$  are infrared-active, the  $A_g + B_g + E_g$  modes are Raman-active, and  $2B_u$  modes are inactive.

Fig. 3 shows the vibrational spectra of a  $\text{AgGa}_5\text{Te}_8$  single crystal. The Raman scattering spectrum exhibits eight bands and is dominated by two strong peaks located at  $125$  and  $141 \text{ cm}^{-1}$  which have the  $A_g$  symmetry. Other Raman and infrared-active modes are tentatively assigned as reported in Table I. It should be noted that the frequencies of the most intense mode in the spectra of  $\text{AgGa}_5\text{Te}_8$  ( $125 \text{ cm}^{-1}$ ) and  $\text{AgGaTe}_2$  ( $129 \text{ cm}^{-1}$ ) nearly coincide with each other. These modes coincide also with the strongest band in the Raman spectrum of  $\text{Ga}_2\text{Te}_3$  [28]. This fact indicates that both modes are attributed mainly to antiphase displacements of tetrahedrally coordinated Ga atoms at nearly identical force coupling constants.

### 3.3. Electrical properties

In this section, we present results of experimental studies concerning the electrical properties to obtain additional information about the nature of the conduction mechanism in Ag-Ga-Te compounds. The electrical measurements have been carried out on single crystals which exhibit a semiconducting n-type

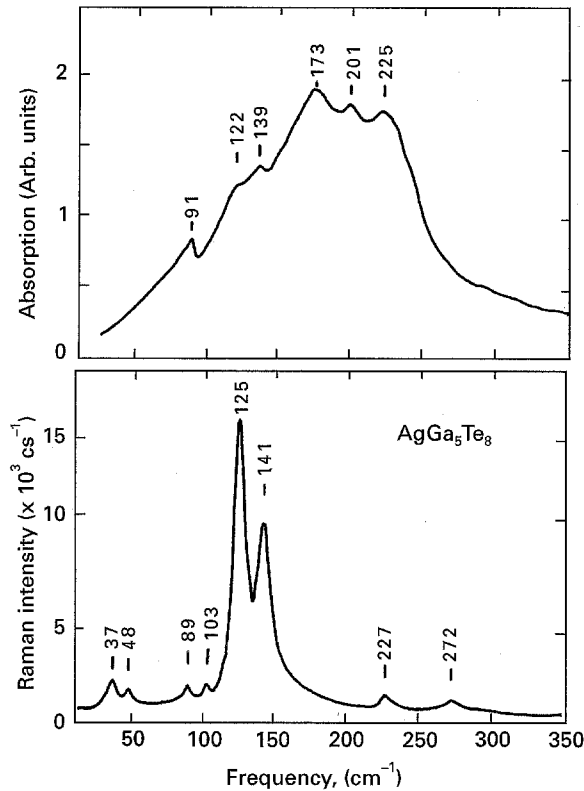


Figure 3 Raman scattering and far-infrared absorption spectra of an  $\text{AgGa}_5\text{Te}_8$  single crystal recorded at room temperature.

conductivity. The temperature dependence of the conductivity for single crystals of  $\text{AgGa}_5\text{Te}_8$  and  $\text{AgGaTe}_2$  are shown in Figs. 4 and 5.

Electrical conduction can take place by two parallel processes: (1) by band conduction and (2) by hopping conduction in the localized states. The former tends to occur at higher temperatures, where carriers excited beyond the mobility edges into non-localized states dominate the transport, while the latter may be due to carriers excited into localized states at band edges [29], that is,

$$\sigma = \sigma_i + \sigma_h, \quad (3)$$

where  $\sigma_i$  is the intrinsic conductivity and  $\sigma_h$  the hopping conductivity. The intrinsic conductivity is of Arrhenius type expressed as;

$$\sigma_i = \sigma_0 \exp(-E_a/k_B T), \quad (4)$$

where  $E_a$  is the thermal activation energy of conductivity. A plot of  $\ln \sigma_i$  versus  $1/T$  gives the thermal activation energy  $E_a$ . From the Arrhenius plot (Fig. 4), the intrinsic conduction gives a thermal activation energy,  $E_a$ , of 0.215 and 0.516 eV for  $\text{AgGaTe}_2$  and  $\text{AgGa}_5\text{Te}_8$ , respectively. Measurements at 450 K showed that samples of both compounds have an electrical conductivity of the order of  $10^{-4} \text{ S cm}^{-1}$ .

A hopping conduction is observed at low temperature in the range below 150 K. The intermediate regime of conduction appears in the temperature range 350–150 K where the activation energy is  $E_a = 0.155 \text{ eV}$  in  $\text{AgGaTe}_2$ . The exact nature of the defects in  $\text{AgGa}_5\text{Te}_8$  remains uncertain but from structural considerations, vacancies seem to play an

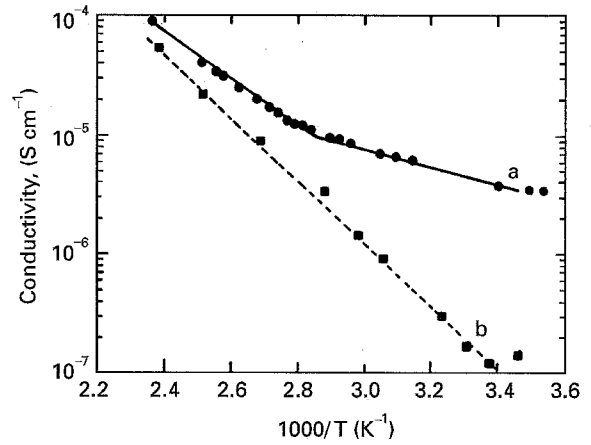


Figure 4 Arrhenius plots of the electrical conductivity of (a)  $\text{AgGaTe}_2$  and (b)  $\text{AgGa}_5\text{Te}_8$  crystals in the region of the intrinsic conductivity.

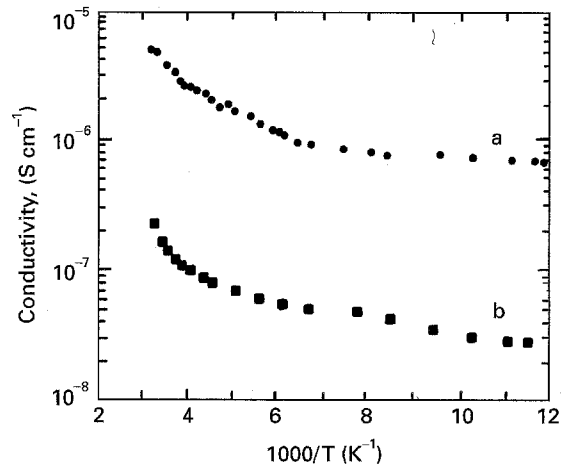


Figure 5 Arrhenius plots of the electrical conductivity of (a)  $\text{AgGaTe}_2$  and (b)  $\text{AgGa}_5\text{Te}_8$  crystals in the low-temperature region.

important role in the conduction mechanism. The low-temperature measurements show that conductivity should be governed by the disordered vacancies in both materials.

As can be seen in Fig. 5 the change in slope of the temperature dependence of conductivity occurs at approximately  $T \approx \theta_D$  where  $\theta_D$  is the Debye temperature. If we assume that the thermal hopping conduction is assisted by the dominant phonon of the A-symmetry type, we can estimate  $\theta_D = 170 \text{ K}$ . Thus the small activation energy value,  $E_a = 11 \text{ meV}$  which is very close to the energy of such a lattice mode,  $\hbar\omega_0 = 0.015 \text{ eV}$  could be an indication for a thermally assisted hopping conduction mechanism in the low-temperature range.

#### 4. Conclusions

(1) The presence of a slight amount of oxygen during the preparation of  $\text{Ag}_2\text{Te}-\text{Ga}_2\text{Te}_3$  compounds creates changes in the phase diagram and the formation of  $\text{AgGa}_5\text{Te}_8$ .

(2) There is a good agreement between experimental and theoretical values of the Raman and infrared-active mode frequencies in  $\text{AgGaTe}_2$ . The

small deviation observed for the Raman-active mode of  $B_1$  symmetry could be due to a slight distortion of the crystal structure.

(3) Raman and infrared spectra of  $AgGa_5Te_8$  have been investigated for the first time. Vibrational modes have been tentatively assigned according to the space group symmetry  $I4_1/a$ .

(4) Electrical measurements showed that the intrinsic conductivity is thermally activated with an activation energy of 0.215 and 0.516 eV for  $AgGaTe_2$  and  $AgGa_5Te_8$ , respectively. In the low-temperature regime, one observes a thermally assisted hopping conduction mechanism which could be due to the presence of stoichiometric vacancies in these compounds.

## References

1. A. MILLER, A. MACKINNON and D. WEAIRE, *Solid State Phys.* **36** (1981) 119.
2. G. D. BOYD, H. M. KASPOER and J. H. MCFEE, *IEEE J. Quantum Electron.* **7** (1971) 563.
3. D. S. CHEMLA, P. J. KUPCEK, D. S. ROBERTSON and R. C. SMITH, *Opt. Commun.* **3** (1971) 29.
4. H. HAHN, G. FRANK, W. KLINGER, A. D. MEYER and G. STORGER, *Z. Anorg. Chem.* **271** (1953) 153.
5. V. GLAZOV, M. S. MIIRGALOVSKAYA and L. A. PETRAKOVA, *Izv. Akad. Nauk. SSSR Tekn.* **10** (1957) 68.
6. V. P. ZHUZE, V. M. SERGEEVA and E. L. SHTRUM, *Soviet Phys. Techn.* **3** (1958) 1925.
7. L. I. BERGER and A. E. BALANEVSKAYA, *Neorg. Mat.* **2** (1966) 1514.
8. L. S. PALATNIK and E. K. BELOVA, *ibid.* **2** (1966) 1025.
9. *Idem*, *ibid.* **3** (1967) 967.
10. *Idem*, *ibid.* **3** (1967) 2194.
11. K. J. RANGE, G. ENGERT and A. WEISS, *Z. Naturforsch* **24B** (1969) 1061.
12. G. KANELLIS, C. KAMPAS and J. SPYRIDELLIS, *Mat. Res. Bull.* **11** (1976) 429.
13. P. KISTAIAH, Y. C. VENUDHAR, K. M. SATHYANARAYANA, L. IYENGAR and K. V. K. RAO, *J. Appl. Cryst.* **14** (1981) 281.
14. M. GUITTARD, C. CARCALY, E. BARTHELEMY, A. MAZURIER, G. KELLER and J. FLAHAUT, *C.R. Acad. Sci. Ser. II (France)* **296** (1983) 973.
15. A. MAZURIER, S. JAULMES and M. GUITTARD, *C.R. Acad. Sci. Ser. II (France)* **299** (1984) 861.
16. V. KRAMER, H. HIRTH, W. HOFFERR and H. P. TRAH, *Thermochim. Acta* **112** (1987) 89.
17. M. GUITTARD, A. MAZURIER, J. RIVET, S. JAULMES, P. H. FOURCROY and A. CHILOUET, *Mat. Res. Bull.* **23** (1988) 217.
18. M. GUITTARD, J. RIVET, F. ALAPINI, A. CHILOUET and A. M. LOIREAU-LOZACH, *J. Less-Common Metals* **170** (1991) 373.
19. C. JULIEN, in "Microionics", edited by M. Balkanski (North-Holland, Amsterdam, 1991) p. 197.
20. I. P. KAMINOW, E. BUEHLER and J. H. WERNICK, *Phys. Rev. B* **2** (1970) 960.
21. G. D. HOLAH, J. S. WEBB and H. J. MONTGOMERY, *J. Phys. C* **7** (1974) 3875.
22. W. H. HOSCHEL, V. HOHLER, A. RAUBER and J. BAARS, *Solid State Commun.* **13** (1973) 1011.
23. J. BAARS and W. H. HOSCHEL, *Solid State Commun.* **11** (1972) 1513.
24. G. K. KANELLIS and K. KAMPAS, *J. Phys.* **38** (1977) 833.
25. G. K. KANELLIS, in "Lattice Dynamics", edited by M. Balkanski (Flammarion, Paris, 1978) p. 99.
26. G. BRANDT, A. RAUBER and J. SCHNEIDER, *Solid State Commun.* **12** (1973) 481.
27. H. POULET and J. P. MATHIEU, *J. Raman Spectroscopy* **2** (1974) 81.
28. C. JULIEN, I. IVANOV, C. ECREPONT and M. GUITTARD, *Phys. Status Solidi* **145** (1994) 207.
29. I. G. AUSTIN and N. F. MOTT, *Adv. Phys.* **18** (1969) 41.

Received 3 June 1994

and accepted 1 December 1995